

TTP00-09  
 HET-BNL-00/8  
 May 2000  
 hep-ph/0005139

# Quartic mass corrections to $R_{\text{had}}$ at $\mathcal{O}(\alpha_s^3)$

K.G. Chetyrkin<sup>a</sup>, R.V. Harlander<sup>b</sup>, and J.H. Kühn<sup>a</sup>

<sup>a</sup>*Institut für Theoretische Teilchenphysik, Universität Karlsruhe,  
 D-76128 Karlsruhe, Germany*

<sup>b</sup>*Brookhaven National Laboratory, Upton, New York 11973*

## Abstract

The total cross section for the production of massive quarks in electron positron annihilation can be predicted in perturbative QCD. After expansion in  $m^2/s$  the quartic terms, i.e. those proportional to  $m^4/s^2$ , are calculated up to order  $\alpha_s^3$  for vector and axial current induced rates. Predictions relevant for charm, bottom and top quarks production are presented. The  $\alpha_s^3$  corrections are shown to be comparable to terms of order  $\alpha_s$  and  $\alpha_s^2$ . As a consequence, the predictions exhibit a sizeable dependence on the renormalization scale. The stability of the prediction is improved and, at the same time, the relative size of the large order terms decreases by replacing the running mass  $\bar{m}(\mu)$  with the scheme independent invariant one  $\hat{m}$ . By combining these results with the prediction for massless case and the quadratic mass terms the cross section for massive quark production at electron positron colliders is put under control in order  $\alpha_s^3$  from the high energy region down to fairly low energies.

The total cross section for hadron production in electron-positron annihilation is one of the most fundamental observables in particle physics. For energies sufficiently far above threshold it can be predicted by perturbative QCD, and it is well accessible experimentally from threshold up to the highest energies of LEP and a future linear collider. It allows for a precise determination of the strong coupling  $\alpha_s$  and, once precision measurements at different energies are available, for a test of its evolution dictated by the renormalization group equation. In many cases the cms energy is far larger than the quark masses which motivated the original calculations to be performed in the idealized case with the masses set to zero from the start. In this limit, the results of  $\mathcal{O}(\alpha_s^2)$  [1] and  $\mathcal{O}(\alpha_s^3)$  [2] were obtained more than two and nearly one decade ago, respectively (for a review see [3]).

However, in a number of interesting cases quark masses do play an important role [3]. For  $Z$  decays into bottom quarks the mass effects have to be included as a consequence of the extremely precise measurements. Bottom quark production at lower energies is affected from production threshold up to a few tens of GeV. Other cases of interest [4,5] are charm production between roughly 5 and 10 GeV and, last but not least, top quark production at a future linear collider [6].

In two-loop approximation the full mass dependence of the cross section has been evaluated since long and, exploiting the optical theorem, both real and imaginary parts are available [7]. In three loop approximation ( $\mathcal{O}(\alpha_s^2)$ ) the corresponding results were obtained only recently. Two methods have been used for this purpose: the first one is based on the evaluation of a large number of terms for the Taylor series of the polarization function  $\Pi(q^2)$  at  $q^2 = 0$  and an appropriately chosen analytic continuation [8]. The second one is based on the application of the large momentum expansion (see [9] and references therein), which provides an expansion of  $\Pi(q^2)$  in powers  $(m^2/q^2)^n$ , modulo logarithms [10]. From the comparison between full result and expansion one learns that the first few terms of the high energy expansion provide a remarkably good description of the full result, from high energies down to values of  $2m/\sqrt{s} = 0.65 - 0.75$ . The existence of the four quark threshold at  $\sqrt{s} = 4m$  and of a corresponding branching point for the polarization function suggests that the high energy expansion diverges for  $\sqrt{s}$  below  $4m$ . Nevertheless, numerical studies [10] as well as qualitative arguments demonstrate that the sum of the first two or three terms of the expansion can be trusted even down to  $3m$  or even, with some optimism,  $2.5m$  (where  $m$  stands for the pole mass).

These considerations pave the way to a prediction of  $R(s)$  including the quark mass dependence to  $\mathcal{O}(\alpha_s^3)$  along the following route: In addition to the massless result the  $m^2/s$  terms of  $\mathcal{O}(\alpha_s^3)$  have been calculated for the absorptive part nearly a decade ago [11]. They were obtained by reconstructing the logarithmic  $\alpha_s^3 m^2/s$  terms of  $\Pi(q^2)$  from the full three loop  $\mathcal{O}(\alpha_s^2 m^2/s)$  result of [12] with the help of the renormalization group equations. These are sufficient to calculate the  $m^2/s$  terms of the imaginary part in the time-like region. The result is cast into a particularly compact form once expressed in terms of the running mass  $m(\mu^2)$ , with the 't Hooft scale  $\mu$  set to  $\sqrt{s}$  throughout [13], since this choice eliminates all terms  $\propto \ln(s/m^2)$ . A generalization of this approach has been formulated for the quartic mass terms in [14, 15] and was originally adopted for the calculation of  $\alpha_s^2 m^4/s^2$  terms. It is based on the operator product expansion and the usage of the renormalization group equation to again construct the logarithmic terms of the polarization function. In addition to the anomalous mass dimension and the  $\beta$ -function the anomalous dimensions of the operators of dimension four are required in appropriate order.

This method also allows to determine the  $\alpha_s^3 m^4/s^2$  terms. The calculation can be reduced to the evaluation of massless propagators and massive tadpole integrals, both at most in three loop approximation. Details of the calculation will be given elsewhere [16]. Compared to the case of the  $m^2/s$  terms an important difference arises: Even adopting the  $\overline{\text{MS}}$  definition (at scale  $\mu^2 = s$ ) for the quark mass, logarithmic terms  $\propto \ln(s/m^2)$  remain in order  $\alpha_s^2$  and above. The power of these logarithms, however, is reduced by one. In fact, these logs may be also summed up (see Refs. [17, 14]).

To predict the  $R$  ratio, it is well justified to consider only one quark as massive and to neglect the masses of the lighter quarks. The heavier quarks decouple (apart from the tiny axial-vector singlet contribution — see below) and can therefore be omitted in the calculations. The massive quark will generically be denoted by  $Q$  in the following, while  $q$  refers to all the lighter quarks.

In the energy region where quark mass effects are relevant, charm and bottom production is solely induced by the electromagnetic vector current. Top quark production, however, which sets in above 350 GeV, receives additional contributions from the axial current. Both vector and axial-vector will be considered separately in the following. The prediction for

both of them is conveniently split up as follows:

$$R^{(v)} = 3 \left( \sum_q v_q^2 r_q + v_Q^2 r_Q^{(v)} + r_{\text{sing}}^{(v)} \right), \quad (1)$$

and similarly for the axial-vector part ( $v \rightarrow a$ ). The sum runs over all massless quark flavors.  $v_{q/Q}$  ( $a_{q/Q}$ ) is the coupling constant to the light/heavy quarks in the vector (axial-vector) case. For low energies only the electromagnetic current contributes,  $v \rightarrow e$  and  $a \rightarrow 0$ . For high energies, both the electromagnetic and neutral current pieces are relevant and have to be included with appropriate weights (see, e.g., [18]).  $r_q$  and  $r_Q^{(v/a)}$  represent the non-singlet contributions arising from diagrams where the external currents are linked by a common quark line. They originate from two different types of diagrams: For  $r_q$  the external current couples to massless quarks; the massive quark then only appears through its coupling to virtual gluons.  $r_q$  is the same for external vector and axial-vector currents. On the other hand,  $r_Q^{(v/a)}$  corresponds to diagrams where the external current couples to the massive quark.  $r_{\text{sing}}^{(v/a)}$ , finally, comprises massless and massive singlet contributions, where either of the external currents is coupled to a separate closed quark line.

Both  $r_q$  and  $r_Q^{(v/a)}$  are written as series in  $m_Q^2/s$ , where  $s$  is the cms energy and  $m_Q$  is the  $\overline{\text{MS}}$  mass of the quark  $Q$ :

$$r_q = r_0 + r_{q,2} + r_{q,4} + \dots, \quad r_Q^{(v/a)} = r_0 + r_{Q,2}^{(v/a)} + r_{Q,4}^{(v/a)} + \dots. \quad (2)$$

$r_0$  denotes the massless approximation, while  $r_{q,n}$  and  $r_{Q,n}^{(v/a)}$  are the mass terms of order  $m_Q^n$ . If not stated otherwise, the renormalization scale  $\mu^2 = s$  is adopted below.

Denoting  $n_f$  the number of active flavors, the massless terms are given by (all the following formulæ are valid up to  $\mathcal{O}(\alpha_s^3)$  unless indicated otherwise)

$$\begin{aligned} r_0 &= 1 + \frac{\alpha_s}{\pi} + \left( \frac{\alpha_s}{\pi} \right)^2 \left[ \frac{365}{24} - 11\zeta_3 + n_f \left( -\frac{11}{12} + \frac{2}{3}\zeta_3 \right) \right] \\ &\quad + \left( \frac{\alpha_s}{\pi} \right)^3 \left[ \frac{87029}{288} - \frac{121}{8}\zeta_2 - \frac{1103}{4}\zeta_3 + \frac{275}{6}\zeta_5 \right. \\ &\quad \left. + n_f \left( -\frac{7847}{216} + \frac{11}{6}\zeta_2 + \frac{262}{9}\zeta_3 - \frac{25}{9}\zeta_5 \right) + n_f^2 \left( \frac{151}{162} - \frac{1}{18}\zeta_2 - \frac{19}{27}\zeta_3 \right) \right] \\ &\approx 1 + \frac{\alpha_s}{\pi} + \left( \frac{\alpha_s}{\pi} \right)^2 (1.98571 - 0.115295 n_f) \\ &\quad + \left( \frac{\alpha_s}{\pi} \right)^3 (-6.63694 - 1.20013 n_f - 0.00517836 n_f^2). \end{aligned} \quad (3)$$

The quadratic mass corrections, separated according to (1), read [11, 19]:

$$\begin{aligned} r_{q,2} &= \frac{m_Q^2}{s} \left( \frac{\alpha_s}{\pi} \right)^3 \left[ -80 + 60\zeta_3 + n_f \left( \frac{32}{9} - \frac{8}{3}\zeta_3 \right) \right] \\ &\approx \frac{m_Q^2}{s} \left( \frac{\alpha_s}{\pi} \right)^3 \left[ -7.87659 + 0.35007 n_f \right], \end{aligned} \quad (4)$$

$$r_{Q,2}^{(v)} = \frac{m_Q^2}{s} \left[ 12 \frac{\alpha_s}{\pi} + \left( \frac{\alpha_s}{\pi} \right)^2 \left( \frac{253}{2} - \frac{13}{3} n_f \right) \right] \quad (5)$$

$$\begin{aligned}
& + \left( \frac{\alpha_s}{\pi} \right)^3 \left( 2442 - \frac{855}{2} \zeta_2 + \frac{490}{3} \zeta_3 - \frac{5225}{6} \zeta_5 \right. \\
& \quad \left. + n_f \left( -\frac{4846}{27} + 34 \zeta_2 - \frac{466}{27} \zeta_3 + \frac{1045}{27} \zeta_5 \right) + n_f^2 \left( \frac{125}{54} - \frac{2}{3} \zeta_2 \right) \right) \Big] \\
\approx & \frac{m_Q^2}{s} \left[ 12 \frac{\alpha_s}{\pi} + \left( \frac{\alpha_s}{\pi} \right)^2 \left( 126.5 - 4.33333 n_f \right) \right. \\
& \quad \left. + \left( \frac{\alpha_s}{\pi} \right)^3 \left( 1032.14 - 104.167 n_f + 1.21819 n_f^2 \right) \right], 
\end{aligned}$$

$$\begin{aligned}
r_{Q,2}^{(a)} = & \frac{m_Q^2}{s} \left[ -6 - 22 \frac{\alpha_s}{\pi} + \left( \frac{\alpha_s}{\pi} \right)^2 \left( -\frac{8221}{24} + 57 \zeta_2 + 117 \zeta_3 \right. \right. \\
& \quad \left. + n_f \left( \frac{151}{12} - 2 \zeta_2 - 4 \zeta_3 \right) \right) \\
& \quad + \left( \frac{\alpha_s}{\pi} \right)^3 \left( -\frac{4613165}{864} + 1340 \zeta_2 + \frac{121075}{36} \zeta_3 - 1270 \zeta_5 \right. \\
& \quad \left. + n_f \left( \frac{72197}{162} - \frac{209}{2} \zeta_2 - \frac{656}{3} \zeta_3 + 5 \zeta_4 + 55 \zeta_5 \right) \right. \\
& \quad \left. + n_f^2 \left( -\frac{13171}{1944} + \frac{16}{9} \zeta_2 + \frac{26}{9} \zeta_3 \right) \right] \tag{6}
\end{aligned}$$

$$\begin{aligned}
\approx & \frac{m_Q^2}{s} \left[ -6 - 22 \frac{\alpha_s}{\pi} + \left( \frac{\alpha_s}{\pi} \right)^2 \left( -108.140 + 4.48524 n_f \right) \right. \\
& \quad \left. + \left( \frac{\alpha_s}{\pi} \right)^3 \left( -409.247 + 73.3578 n_f - 0.378270 n_f^2 \right) \right]. \tag{7}
\end{aligned}$$

The quadratic mass terms in  $r_q$  contribute in  $\mathcal{O}(\alpha_s^3)$  and higher only [11]. Finally, we present the quartic mass corrections up to  $\mathcal{O}(\alpha_s^3)$ :

$$\begin{aligned}
r_{q,4} = & \left( \frac{m_Q^2}{s} \right)^2 \left[ \left( \frac{\alpha_s}{\pi} \right)^2 \left( \frac{13}{3} - l_{ms} - 4 \zeta_3 \right) \right. \\
& \quad + \left( \frac{\alpha_s}{\pi} \right)^3 \left( -\frac{9707}{144} + 2 l_{ms}^2 + 15 \zeta_2 + 25 \zeta_3 + \frac{50}{3} \zeta_5 + l_{ms} \left( \frac{43}{12} - 22 \zeta_3 \right) \right. \\
& \quad \left. + n_f \left( \frac{457}{108} - \frac{2}{3} \zeta_2 - \frac{22}{9} \zeta_3 + l_{ms} \left( -\frac{13}{18} + \frac{4}{3} \zeta_3 \right) \right) \right] \tag{8} \\
\approx & \left( \frac{m_Q^2}{s} \right)^2 \left[ \left( \frac{\alpha_s}{\pi} \right)^2 \left( -0.474894 - l_{ms} \right) \right. \\
& \quad + \left( \frac{\alpha_s}{\pi} \right)^3 \left( 4.59784 - 22.8619 l_{ms} + 2 l_{ms}^2 \right. \\
& \quad \left. \left. + (0.196497 + 0.88052 l_{ms}) n_f \right) \right],
\end{aligned}$$

$$\begin{aligned}
r_{Q,4}^{(v)} = & \left( \frac{m_Q^2}{s} \right)^2 \left[ -6 - 22 \frac{\alpha_s}{\pi} + \left( \frac{\alpha_s}{\pi} \right)^2 \left( -\frac{2977}{12} + 162 \zeta_2 + 108 \zeta_3 - \frac{13}{2} l_{ms} \right. \right. \\
& \quad \left. + n_f \left( \frac{143}{18} + \frac{1}{3} l_{ms} - 4 \zeta_2 - \frac{8}{3} \zeta_3 \right) \right)
\end{aligned}$$

$$\begin{aligned}
& + \left( \frac{\alpha_s}{\pi} \right)^3 \left( -\frac{1274461}{432} + \frac{12099}{4} \zeta_2 + \frac{64123}{18} \zeta_3 - \frac{13285}{9} \zeta_5 \right. \\
& + l_{ms} \left( -\frac{1309}{6} - 22 \zeta_3 \right) + 13 l_{ms}^2 + n_f \left( \frac{130009}{648} - \frac{574}{3} \zeta_2 - \frac{1672}{9} \zeta_3 \right. \\
& + 10 \zeta_4 + \frac{440}{9} \zeta_5 + l_{ms} \left( \frac{199}{12} + \frac{4}{3} \zeta_3 \right) - \frac{2}{3} l_{ms}^2 \left. \right) \\
& \left. + n_f^2 \left( -\frac{463}{972} + \frac{23}{9} \zeta_2 + \frac{28}{27} \zeta_3 - \frac{5}{27} l_{ms} \right) \right) \quad (9)
\end{aligned}$$

$$\begin{aligned}
\approx & \left( \frac{m_Q^2}{s} \right)^2 \left[ -6 - 22 \frac{\alpha_s}{\pi} \right. \\
& + \left( \frac{\alpha_s}{\pi} \right)^2 (148.218 - 6.5 l_{ms} + (-1.84078 + 0.333333 l_{ms}) n_f) \\
& + \left( \frac{\alpha_s}{\pi} \right)^3 (4776.95 - 244.612 l_{ms} + 13 l_{ms}^2 \\
& + (-275.898 + 18.1861 l_{ms} - 0.666667 l_{ms}^2) n_f \\
& \left. + (4.97396 - 0.185185 l_{ms}) n_f^2 \right],
\end{aligned}$$

$$\begin{aligned}
r_{Q,4}^{(a)} = & \left( \frac{m_Q^2}{s} \right)^2 \left[ 6 + 10 \frac{\alpha_s}{\pi} + \left( \frac{\alpha_s}{\pi} \right)^2 \left( \frac{1147}{4} - 162 \zeta_2 - 224 \zeta_3 + \frac{75}{2} l_{ms} \right. \right. \\
& + n_f \left( -\frac{41}{6} + 4 \zeta_2 + \frac{16}{3} \zeta_3 - \frac{7}{3} l_{ms} \right) \left. \right) \\
& + \left( \frac{\alpha_s}{\pi} \right)^3 \left( \frac{222517}{48} - \frac{10881}{4} \zeta_2 - \frac{20147}{6} \zeta_3 - \frac{2225}{3} \zeta_5 \right. \\
& + l_{ms} \left( \frac{4385}{6} - 22 \zeta_3 \right) - 75 l_{ms}^2 \\
& + n_f \left( -\frac{200923}{648} + 196 \zeta_2 + \frac{5002}{27} \zeta_3 - 10 \zeta_4 + \frac{1040}{27} \zeta_5 \right. \\
& + l_{ms} \left( -\frac{2323}{36} + \frac{4}{3} \zeta_3 \right) + \frac{14}{3} l_{ms}^2 \left. \right) \\
& \left. + n_f^2 \left( \frac{2995}{972} - \frac{29}{9} \zeta_2 - \frac{20}{27} \zeta_3 + \frac{23}{27} l_{ms} \right) \right) \quad (10)
\end{aligned}$$

$$\begin{aligned}
\approx & \left( \frac{m_Q^2}{s} \right)^2 \left[ 6 + 10 \frac{\alpha_s}{\pi} \right. \\
& + \left( \frac{\alpha_s}{\pi} \right)^2 \left( -248.99 + 37.5 l_{ms} + (6.15737 - 2.33333 l_{ms}) n_f \right) \\
& + \left( \frac{\alpha_s}{\pi} \right)^3 \left( -4646.22 + 704.388 l_{ms} - 75 l_{ms}^2 \right. \\
& + (264.151 - 62.9250 l_{ms} + 4.66667 l_{ms}^2) n_f \\
& \left. \left. + (-3.10948 + 0.851852 l_{ms}) n_f^2 \right) \right].
\end{aligned}$$

The singlet contributions in the vector case are numerically small:

$$\begin{aligned}
r_{\text{sing}}^{(v)} &= \left(\frac{\alpha_s}{\pi}\right)^3 \left\{ \left(v_Q + \sum_q v_q\right)^2 \left(\frac{55}{216} - \frac{5}{9}\zeta_3\right) \right. \\
&\quad \left. + \left(\frac{m_Q^2}{s}\right)^2 v_Q \left(v_Q + \sum_q v_q\right) \left(-\frac{20}{9} + \frac{50}{3}\zeta_3\right) \right\} \\
&\approx \left(\frac{\alpha_s}{\pi}\right)^3 \left\{ -0.413180 \left(v_Q + \sum_q v_q\right)^2 \right. \\
&\quad \left. + 17.8121 v_Q \left(v_Q + \sum_q v_q\right) \left(\frac{m_Q^2}{s}\right)^2 \right\} + \mathcal{O}\left(\left(\frac{m_Q^2}{s}\right)^3\right). \quad (11)
\end{aligned}$$

They do not receive  $m^2$  corrections [11].

The singlet contributions in the axial-vector case are exceptional in the sense that for bottom quark production the top quark does not decouple, i.e., the contributions where the top quark couples to one of the external currents are not suppressed by powers of  $1/m_t^2$ . The corresponding corrections up to  $\mathcal{O}(m_b^2\alpha_s^3)$  have been computed in [20–23]. They turn out to be small, so we will neglect them in the following.

Considering the axial vector singlet contribution to top quark production, on the other hand, one should take into account the full top-bottom doublet, because the axial anomaly cancels in this combination. However, this strategy induces completely massless final states without any top quarks. At order  $\alpha_s^2$  the expansion for the contributions from the full top-bottom doublet starts with the  $m^6$  terms [6]. The separate piece from massless cuts is known in analytical form [20] and has to be subtracted if one wants to obtain the contribution from the final states with top quarks. The complete result is given in Ref. [6]. Thus the singlet contribution to  $t\bar{t}$  production is given in expanded form by

$$\begin{aligned}
r_{\text{sing}} &= \frac{1}{4} \left(\frac{\alpha_s}{\pi}\right)^2 \left\{ \frac{5}{4} - \frac{2}{3}\zeta_2 + \frac{m^2}{s} \left( -\frac{4}{3} + \frac{20}{3}\zeta_2 + 4l_{ms} - \frac{2}{3}l_{ms}^2 \right) \right. \\
&\quad \left. + \left(\frac{m^2}{s}\right)^2 \left[ \frac{13}{2} + \frac{2}{3}\zeta_2 - \frac{16}{3}\zeta_3 + l_{ms} \left( -5 + \frac{4}{3}\zeta_2 \right) - \frac{1}{3}l_{ms}^2 - \frac{2}{9}l_{ms}^3 \right] \right\} \\
&\quad + \mathcal{O}(\alpha_s^3) \\
&= \frac{1}{4} \left(\frac{\alpha_s}{\pi}\right)^2 \left[ 0.153377 + \frac{m^2}{s} (9.63289 + 4l_{ms} - 0.666667l_{ms}^2) \right. \\
&\quad \left. + \left(\frac{m^2}{s}\right)^2 (1.18565 - 2.80675l_{ms} - 0.333333l_{ms}^2 - 0.222222l_{ms}^3) \right] \\
&\quad + \mathcal{O}(\alpha_s^3), \quad (12)
\end{aligned}$$

where the weak coupling  $a_t^2 = a_b^2 = -a_t a_b = 1/4$  has been pulled out for clarity. The separate contribution from the massless cuts is not yet available in order  $\alpha_s^3$ . In principle it should be subtracted from the following result in order to arrive at the production rate for top quarks:

$$r'_{\text{sing}} = \frac{1}{4} \left(\frac{\alpha_s}{\pi}\right)^3 \left(\frac{m_t^2}{s}\right)^2 \left[ -\frac{380}{3}\zeta_3 + \frac{1520}{3}\zeta_5 + n_f \left( \frac{40}{9}\zeta_3 - \frac{160}{9}\zeta_5 \right) \right]$$

$\sqrt{s}$	5.	6.	7.	8.	9.	10.	10.5
$\alpha_s^{(4)}(s)$	0.212	0.2	0.192	0.185	0.179	0.174	0.172
$m_c^{(4)}(\sqrt{s})$	0.829	0.803	0.784	0.769	0.756	0.745	0.74

$\sqrt{s}$	11.	12.	14.	16.	20.
$\alpha_s^{(5)}(s)$	0.174	0.171	0.165	0.161	0.153
$m_b^{(5)}(\sqrt{s})$	3.61	3.57	3.5	3.44	3.35

$\sqrt{s}$	420.	460.	500.
$\alpha_s^{(6)}(s)$	0.097	0.0961	0.0952
$m_t^{(6)}(\sqrt{s})$	154.	153.	152.

Table 1: Running coupling and masses at different scales. Matching for  $\alpha_s$  is performed at the values  $m(m)$  given in (14).

$$\approx \frac{1}{4} \left( \frac{\alpha_s}{\pi} \right)^3 \left( \frac{m_t^2}{s} \right)^2 (373.116 - 13.0918 n_f) . \quad (13)$$

The prime indicates that this expression still contains the contributions from purely massless final states, as mentioned before. We explicitly denote the mass by  $m_t$  here in order to recall that, on the one hand, this result applies only to top production, and on the other hand, the full  $(t, b)$  doublet has been taken into account.

Let us now investigate the numerical significance of mass effects for the charm and bottom case. If not stated otherwise, we will adopt the following input data:

$$M_Z = 91.19 \text{ GeV}, \quad \alpha_s(M_Z^2) = 0.118, \\ m_c(m_c) = 1.2 \text{ GeV}, \quad m_b(m_b) = 4.2 \text{ GeV}, \quad m_t(m_t) = 165 \text{ GeV}. \quad (14)$$

The running of the quark masses and the coupling constant to the scale  $\sqrt{s}$  is performed with three loop accuracy. Since we are working in the  $\overline{\text{MS}}$  scheme, we have to take into account the matching conditions for  $\alpha_s^{(n_f)}$  when going from  $n_f$  to  $n_f \pm 1$ . We perform the matching from  $n_f = 5$  to  $n_f = 4$  at  $m_b(m_b)$  and from  $n_f = 5$  to  $n_f = 6$  at  $m_t(m_t)$ . For illustration, some values for  $\alpha_s(s)$ ,  $m_c(\sqrt{s})$ ,  $m_b(\sqrt{s})$ , and  $m_t(\sqrt{s})$  are displayed in Table 1. The charm, bottom, and top masses are defined for  $n_f = 4, 5$ , and  $6$ , respectively. As stated above, the approximation is expected to become unreliable in the threshold region, that means below  $5.5 - 6$  GeV for charm,  $12 - 12.5$  GeV for bottom, and  $420 - 450$  GeV for top contributions, which justifies the choice for the cms energies in the figures presented below.

In Figs. 1–4 we display separately the contributions for the massless case (Fig. 1) and for the  $m^2$  and  $m^4$  terms, including successively higher orders in  $\alpha_s$ . While Fig. 2 shows the effects of the diagrams with light quarks coupling to the external current, Figs. 3 and 4 correspond to the case where the massive quark couples directly to the external current. The axial contribution is presented for the top quark only.

The variation of the prediction with the renormalization scale  $\mu$  is shown in Figs. 5 to 8.

	$\alpha_s^0$	$\alpha_s^1$	$\alpha_s^2$	$\alpha_s^3$	$\Sigma$
$m^0$	1.	0.05482	0.004581	-0.001898	1.058
$m^2$	0	0.003264	0.001628	0.000519	1.063
$m^4$	-0.0001477	-0.00002969	0.00001245	0.00002016	1.063

Table 2:  $r_Q^{(v)}$  for  $\sqrt{s} = 10.5$  GeV.

As discussed already in earlier papers, the size of the higher order corrections decreases quickly with increasing order in  $\alpha_s$ , as far as the massless approximation is concerned (Fig. 1). This is reflected in the stability of the result under variation of the renormalization scale  $\mu$  by a factor between 1/2 and 2 as displayed in Fig. 5. The  $m^2$  terms in  $r_q$  (Fig. 2 (a), (c), (e)) arise for the first time in order  $\alpha_s^3$ . As a consequence this prediction exhibits a strong  $\mu$  dependence as displayed in Fig. 6 (a), (c), and (e). However, this term is typically around  $10^{-4}$  and thus irrelevant for all practical purposes.

The quartic terms in  $r_q$  which are displayed in Figs. 2 (b), (d), and (f) contribute in  $\mathcal{O}(\alpha_s^2)$  and higher. Terms of order  $m^4\alpha_s^3$  and  $m^4\alpha_s^2$  are of comparable magnitude, not only for the low energy case but even at the highest energy, whence the prediction for the  $m^4$  terms in  $r_q$  must be considered as uncertain within a factor two. This is reflected in the strong  $\mu$  dependence of the result shown in Fig. 6 (b), (d), and (e).

No reduction of this variation is observed when moving from the  $\alpha_s^2$  to the  $\alpha_s^3$  calculation. Nevertheless, the prediction for the total cross section is not seriously affected by this instability since these terms are again of order  $10^{-4}$  only and thus far below the foreseeable experimental precision.

The dominant quartic mass terms are obviously expected from  $r_Q$ , the part where the massive quark is coupled to the external current. For comparison we also discuss the quadratic terms which are known since long and are shown in Fig. 3. The vector current induced piece is displayed in Fig. 3 for  $c$ ,  $b$ , and  $t$  quarks, the axial piece is shown for  $t$  quarks only. Terms of increasing order in  $\alpha_s$  decrease in magnitude and apparent convergence is observed. This welcome behavior is reflected by the improved stability of higher orders under variations of  $\mu$  (Fig. 7). The behavior of the quartic terms which are the theme of this paper is more problematic (Fig. 4). The bulk of the result is given by the Born approximation. The order  $\alpha_s$ - $\alpha_s^2$ - and  $\alpha_s^3$ -corrections are significantly smaller than the leading terms. However, with increasing order they do not decrease but remain roughly comparable in magnitude. This is reflected in the strong  $\mu$  dependence displayed in Fig. 8. Depending on the choice of  $\mu$ , the relative size of the three corrections varies drastically.

Nevertheless, the higher orders are small compared to the  $m^4$  Born terms and, even more important, their instability does not affect the stability of the overall prediction for  $R$  resulting from the sum of the different terms. Accepting as an estimate of the uncertainty of  $r_{Q,4}$  its variation with  $\mu$  between  $\sqrt{s}/2$  and  $2\sqrt{s}$ ,  $r_{c,4}$  at 6 GeV varies by  $\pm 0.0005$ ,  $r_{b,4}$  at 14 GeV by  $\pm 0.0016$ . For  $r_{t,4}$  the variation is negligible.

These considerations demonstrate that a prediction for  $R$  has been obtained which is valid in order  $\alpha_s^3$  and includes mass terms in an expansion up to order  $m^4$ .

From a pragmatic point of view the smallness of the  $m^4$  terms, in particular of their QCD

corrections, allows to ignore their apparent instability. Nevertheless, one may also attempt to arrive at a more stable result for the quartic terms by replacing the running mass by the invariant one ( $\hat{m}$ ) through

$$m(\mu) = \hat{m} \exp \int da \frac{\gamma_m(a)}{a\beta(a)}, \quad (15)$$

where  $a \equiv \alpha_s(\mu^2)/\pi$ .  $\beta(a)$  and  $\gamma_m(a)$  are the renormalization group functions governing the running of the strong coupling constant and the quark mass:

$$\mu^2 \frac{d}{d\mu^2} a = a \beta(a), \quad \mu^2 \frac{d}{d\mu^2} m = m \gamma_m(a). \quad (16)$$

Their perturbative expansion is known up to  $\mathcal{O}(\alpha_s^4)$  both for  $\beta(a)$  [24] and  $\gamma_m(a)$  [25]. The integral in (15) is solved perturbatively, and the resulting expression for  $R$  is re-expanded in  $\alpha_s$  up to the third power. For the scale invariant mass we assume the values  $\hat{m}_c = 2.8$  GeV,  $\hat{m}_b = 15.3$  GeV, and  $\hat{m}_t = 1076$  GeV which corresponds to solving (15) w.r.t.  $\hat{m}$  for  $\mu = m$  at three-loop order and using the numerical values of Eq. (14). The result for the  $\mu$  dependence of  $r_{Q,4}^{(v)}$  in this approach is shown in Fig. 9.

The variation of the  $\mathcal{O}(\alpha_s^3)$  prediction with  $\mu$  is reduced. For example, for  $\sqrt{s} = 6$  GeV the  $\mathcal{O}(\alpha_s^3)$  prediction in Fig. 8 varies between  $-0.10 \cdot 10^{-2}$  and  $-0.20 \cdot 10^{-2}$  with a central value of  $-0.18 \cdot 10^{-2}$  at  $\mu = \sqrt{s}$ , compared to a range from  $-0.13 \cdot 10^{-2}$  to  $-0.20 \cdot 10^{-2}$  with a central value of  $-0.19 \cdot 10^{-2}$  in Fig. 9. At the same time one observes a reduction of the higher order terms compared to the Born approximation and the  $\mathcal{O}(\alpha_s)$  prediction. For  $\mu = \sqrt{s}$  the results within the two approaches are quite close, which gives additional confidence in the reliability of these numbers.

## Summary

The total cross section for the production of massive quarks in electron positron annihilation can be predicted in perturbative QCD. After expansion in  $m^2/s$  the quartic terms, i.e. those proportional to  $m^4/s^2$ , were calculated up to order  $\alpha_s^3$  for vector and axial current induced rates. Predictions relevant for charm, bottom and top quark production were presented. The  $\alpha_s^3$  corrections were shown to be comparable to terms of order  $\alpha_s$  and  $\alpha_s^2$ . As a consequence, the predictions exhibit a sizeable dependence on the renormalization scale. Adopting instead of the  $\overline{\text{MS}}$  scheme a framework where the running mass  $\bar{m}(\mu)$  is replaced by the invariant mass  $\hat{m}$ , the stability of the prediction is improved and, at the same time, the relative size of the large order terms decreases. Obviously, an improved understanding of the origin of these large corrections would be highly desirable.

Combining these results with the massless prediction and the quadratic mass terms we have demonstrated that the cross section for massive quark production at electron positron colliders is under control in order  $\alpha_s^3$  from the high energy region down to fairly low energies.

## Acknowledgments

This work was supported by *DFG-Forschergruppe “Quantenfeldtheorie, Computeralgebra und Monte-Carlo-Simulation”*. R.H. acknowledges support by *Landesgraduiertenförderung* at the University of Karlsruhe and by *Deutsche Forschungsgemeinschaft*.

## References

- [1] K.G. Chetyrkin, A.L. Kataev and F.V. Tkachov, *Phys. Lett.* **B 85** (1979) 277; M. Dine and J. Sapirstein, *Phys. Rev. Lett.* **43** (1979) 668; W. Celmaster and R.J. Gonsalves, *Phys. Rev. Lett.* **44** (1980) 560.
- [2] S.G. Gorishny, A.L. Kataev and S.A. Larin, *Phys. Lett.* **B 259** (1991) 144; L.R. Surguladze and M.A. Samuel, *Phys. Rev. Lett.* **66** (1991) 560; (E) *ibid.*, 2416; K.G. Chetyrkin, *Phys. Lett.* **B 391** (1997) 402.
- [3] K.G. Chetyrkin, J.H. Kühn and A. Kwiatkowski, *Phys. Reports* **277** (1997) 189.
- [4] K.G. Chetyrkin and J.H. Kühn, *Phys. Lett.* **B 342** (1995) 356.
- [5] K.G. Chetyrkin, J.H. Kühn, and T. Teubner, *Phys. Rev. D* **56** (1997) 3011.
- [6] R. Harlander and M. Steinhauser, *Eur. Phys. J. C* **2** (1998) 151.
- [7] G. Källen and A. Sabry, *K. Dan. Vidensk. Selsk. Mat.-Fys. Medd.* **29** (1955) No. 17.
- [8] K.G. Chetyrkin, J.H. Kühn, and M. Steinhauser, *Phys. Lett.* **B 371** (1996) 93; *Nucl. Phys.* **B 482** (1996) 213; *Nucl. Phys.* **B 505** (1997) 40.
- [9] V.A. Smirnov, *Mod. Phys. Lett.* **A 10** (1995) 1485; *Renormalization and Asymptotic Expansion* (Birkhäuser, Basel, 1991).
- [10] K.G. Chetyrkin, R. Harlander, J.H. Kühn, and M. Steinhauser, *Nucl. Phys.* **B 503** (1997) 339.
- [11] K.G. Chetyrkin and J.H. Kühn, *Phys. Lett.* **B 248** (1990) 359.
- [12] S.G. Gorishny, A.L. Kataev, and S.A. Larin, *Nuovo Cim.* **92A** (1986) 119.
- [13] G. 't Hooft, *Nucl. Phys.* **B 61** (1973) 455.
- [14] K.G. Chetyrkin and V.P. Spiridonov, *Yad. Fiz.* **47** (1988) 818 (*Sov. J. Nucl. Phys.* **47** (1988) 522).
- [15] K.G. Chetyrkin and J.H. Kühn, *Nucl. Phys.* **B 432** (1994) 337.
- [16] K.G. Chetyrkin, R. Harlander, and J.H. Kühn, in preparation.
- [17] D.J. Broadhurst and S.C. Generalis, Open University preprint OUT-4102-12 (1984).
- [18] J.H. Kühn and P. Zerwas, in: *Advanced Series on Directions in High Energy Physics — Vol. 15, Heavy Flavours II*, Edited by A.J. Buras and M. Lindner, World Scientific, 1997, p 493.
- [19] K.G. Chetyrkin and J.H. Kühn, *Phys. Lett.* **B 406** (1997) 102.
- [20] B.A. Kniehl and J.H. Kühn, *Nucl. Phys.* **B 329** (1990) 547; *Phys. Lett.* **B 224** (1990) 229.
- [21] K.G. Chetyrkin and J.H. Kühn, *Phys. Lett.* **B 308** (1993) 127.

- [22] K.G. Chetyrkin and O.V. Tarasov, *Phys. Lett.* **B 327** (1994) 114;  
S.A. Larin, T. van Ritbergen and J.A.M. Vermaasen, *Phys. Lett.* **B 320** (1994) 159.
- [23] K.G. Chetyrkin and A. Kwiatkowski, *Phys. Lett.* **B 319** (1993) 307; *Phys. Lett.* **B 305** (1993) 285.
- [24] T. van Ritbergen, J.A.M. Vermaasen, and S.A. Larin, *Phys. Lett.* **B 400** (1997) 379.
- [25] K.G. Chetyrkin, *Phys. Lett.* **B 404** (1997) 161;  
J.A.M. Vermaasen, S.A. Larin, and T. van Ritbergen, *Phys. Lett.* **B 404** (1997) 153.

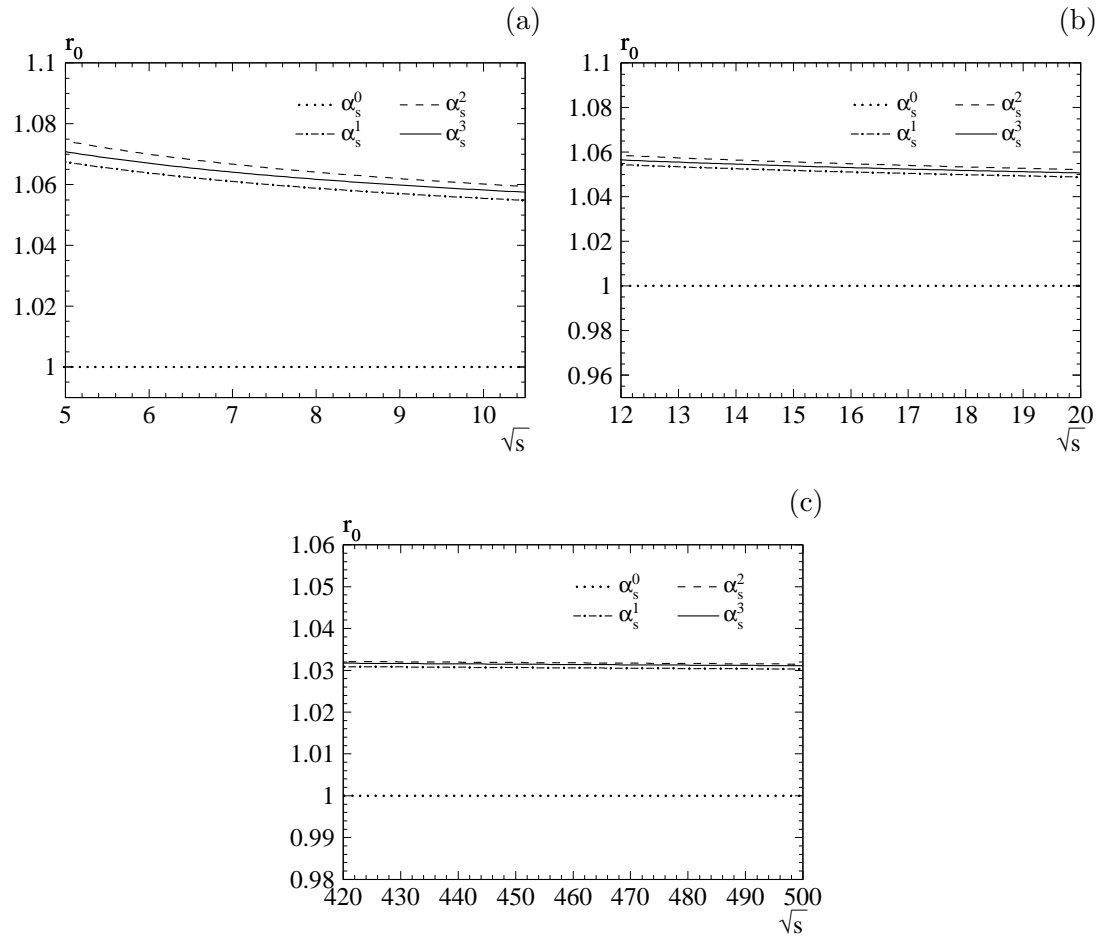


Figure 1: The massless approximation  $r_0$  in three different energy ranges, relevant for (a) charm, (b) bottom and (c) top production.

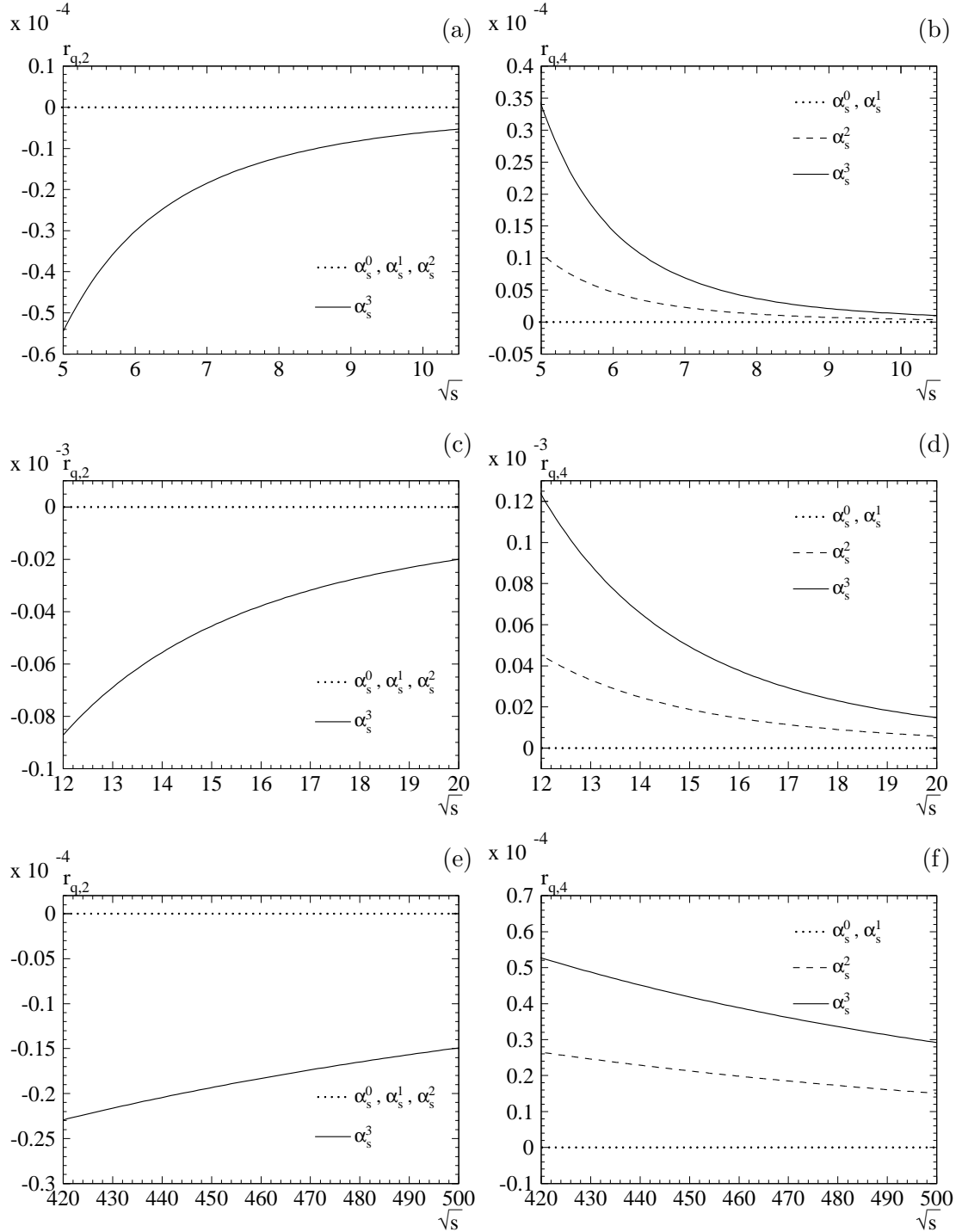


Figure 2: Mass corrections to the non-singlet contribution of  $r_q$  for  $c$ ,  $b$ , and  $t$  production (1., 2., and 3. row, respectively), arising from diagrams where the external current couples to massless quarks only. Left column: quadratic, starting to be non-zero in  $\mathcal{O}(\alpha_s^3)$ ; right column: quartic mass corrections, starting to be non-zero in  $\mathcal{O}(\alpha_s^2)$ .

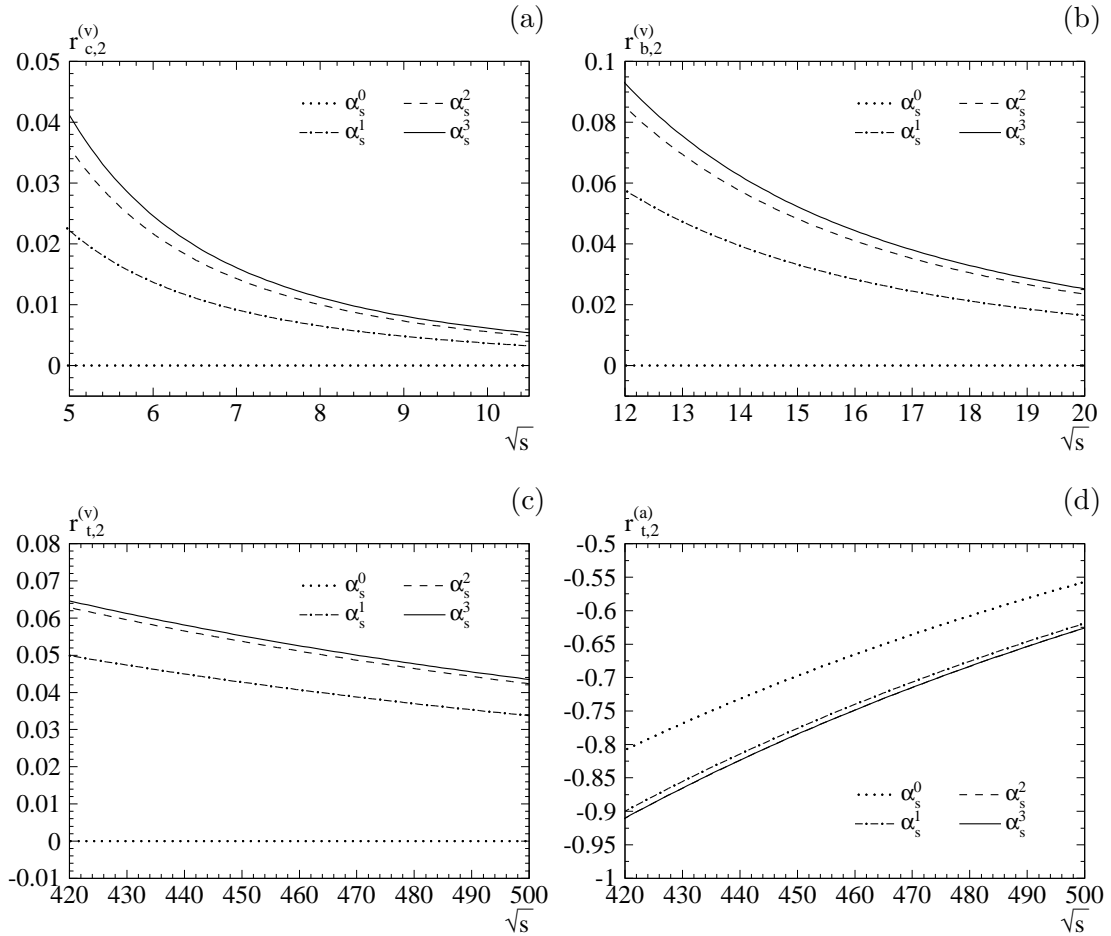


Figure 3: Quadratic mass corrections ( $\propto m^2$ ) to the non-singlet contribution of  $r_Q$  for  $Q = c, b, t$ , arising from diagrams where the external current couples directly to the massive quark. Upper row: vector current for  $c$  and  $b$  quarks; lower row: vector and axial currents for  $t$  quark.

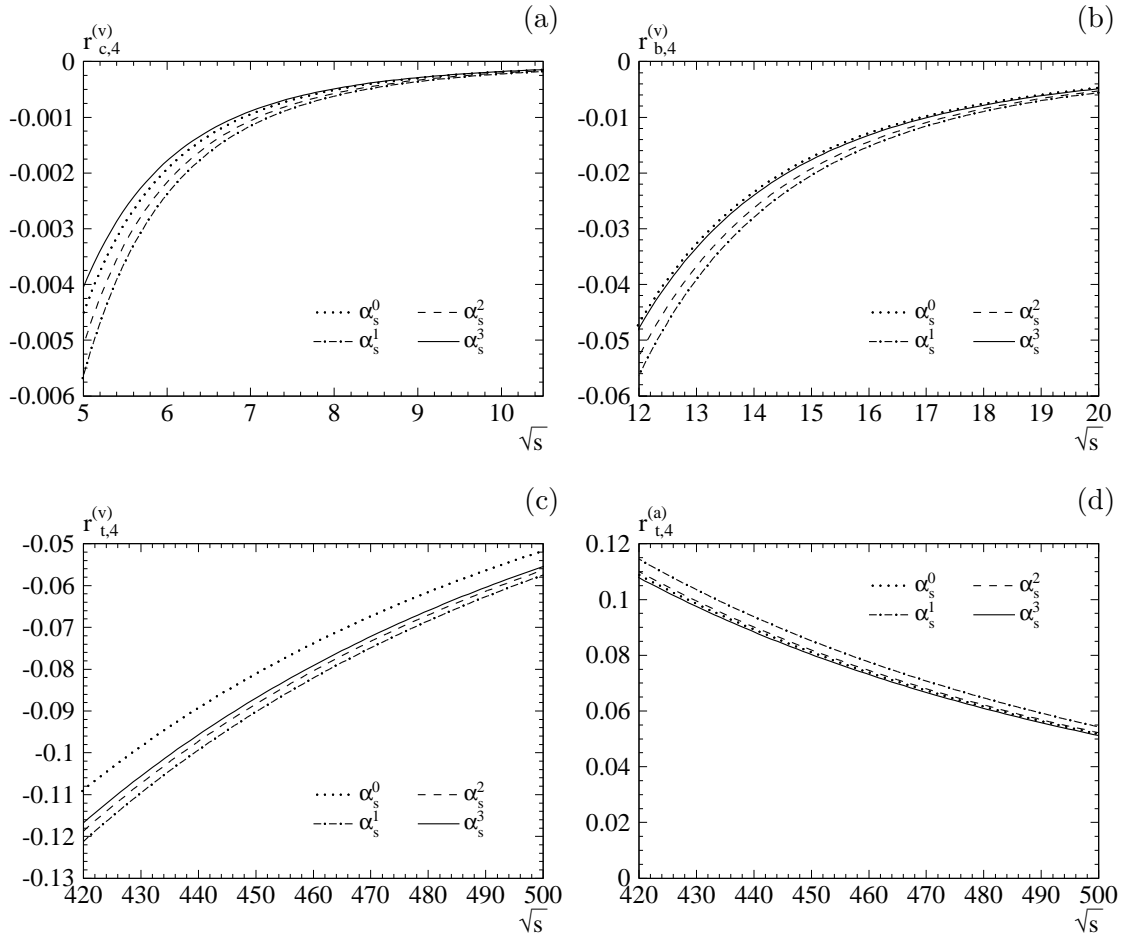


Figure 4: Quartic mass corrections ( $\propto m^4$ ) to the non-singlet contribution of  $r_Q$  for  $Q = c, b, t$ , arising from diagrams where the external current couples directly to the massive quark. Upper row: vector currents for  $c$  and  $b$  quarks; lower row: vector and axial currents for  $t$  quark.

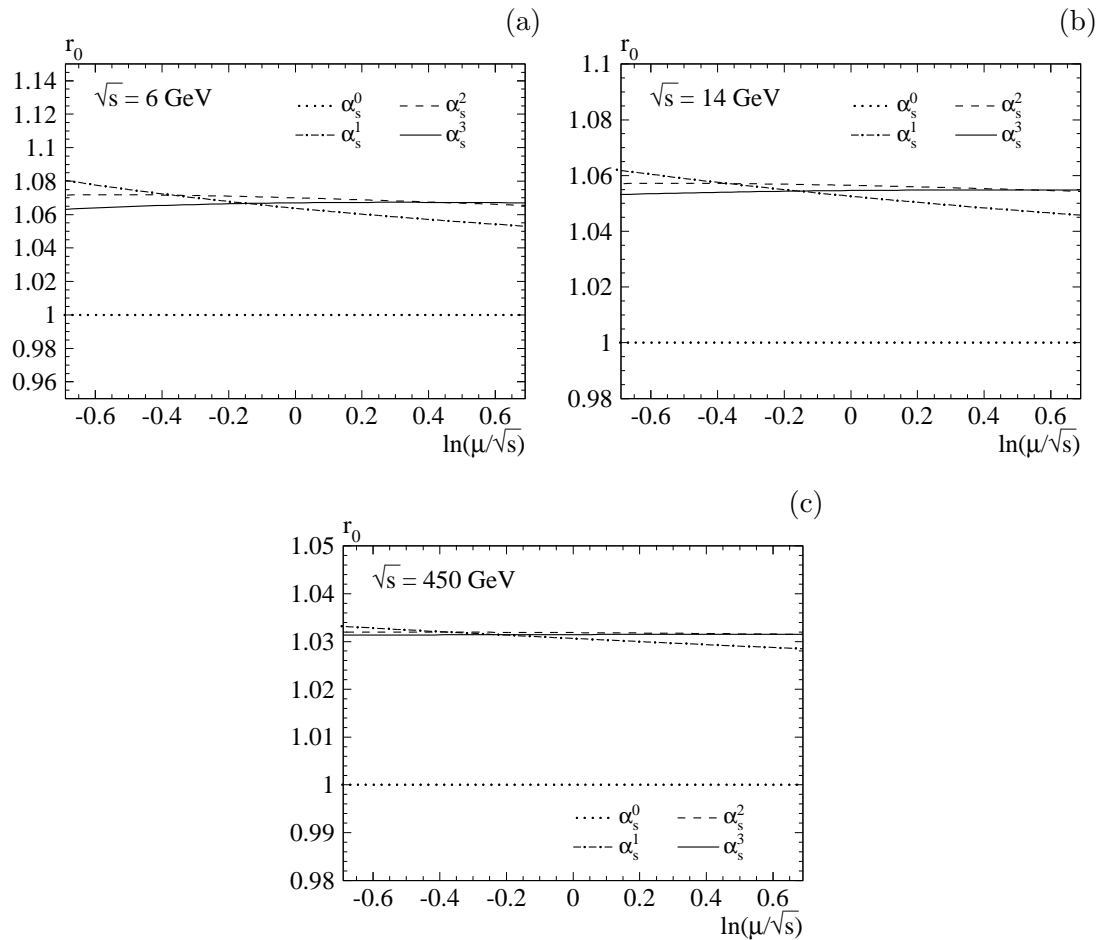


Figure 5: Variation of  $r_0$  with  $\mu$ .  $s$  is fixed to values relevant for the production of (a) charm, (b) bottom, and (c) top quarks. The abscissa ranges from  $\mu = \sqrt{s}/2$  to  $\mu = 2\sqrt{s}$ .

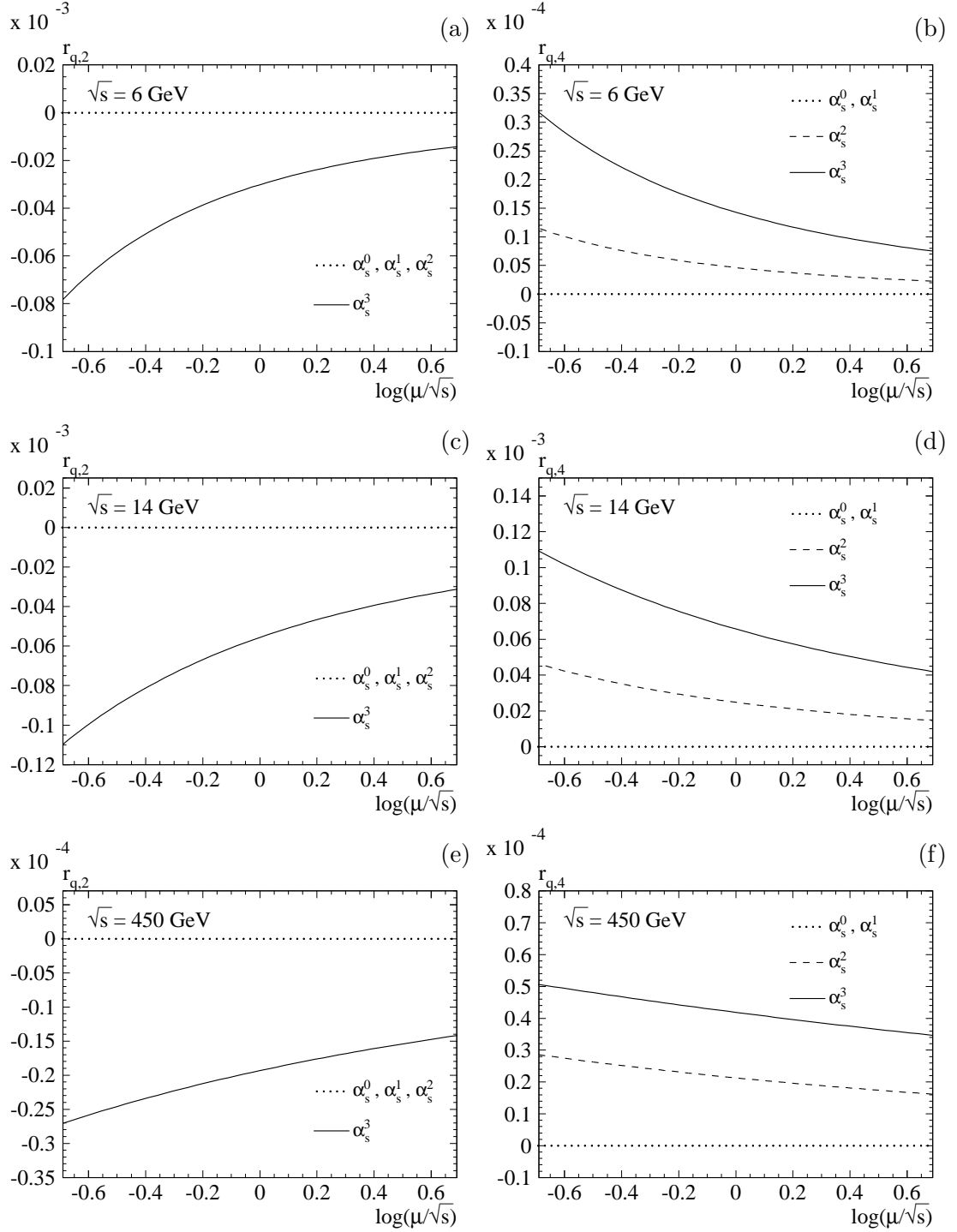


Figure 6: Variation of  $r_{q,2}$  (left column) and  $r_{q,4}$  (right column) with  $\mu$ . The first, second, and third row correspond to charm, bottom, and top production, respectively.

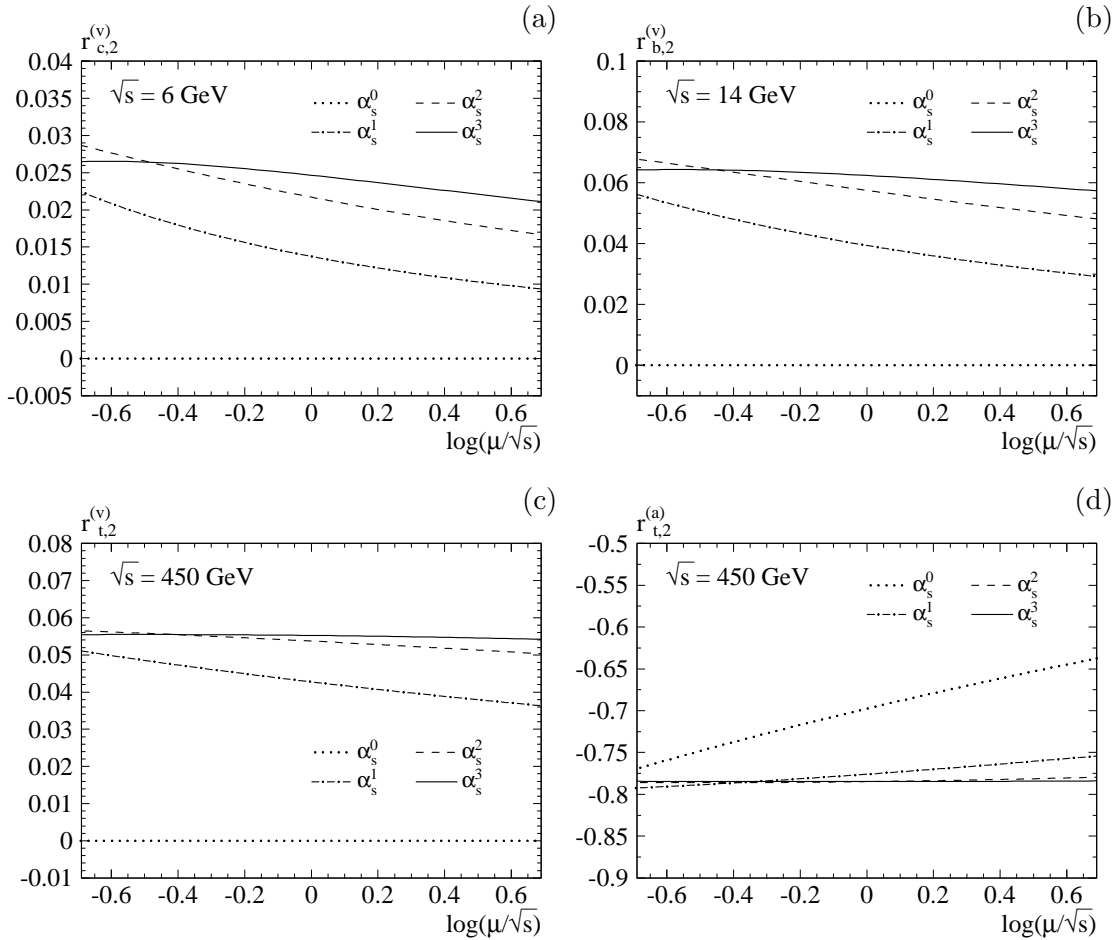


Figure 7: Variation of  $r_{Q,2}^{(v/a)}$  with  $\mu$ . First row: (a) charm, (b) bottom production for vector case; second row: (c) vector and (d) axial-vector case for top production.

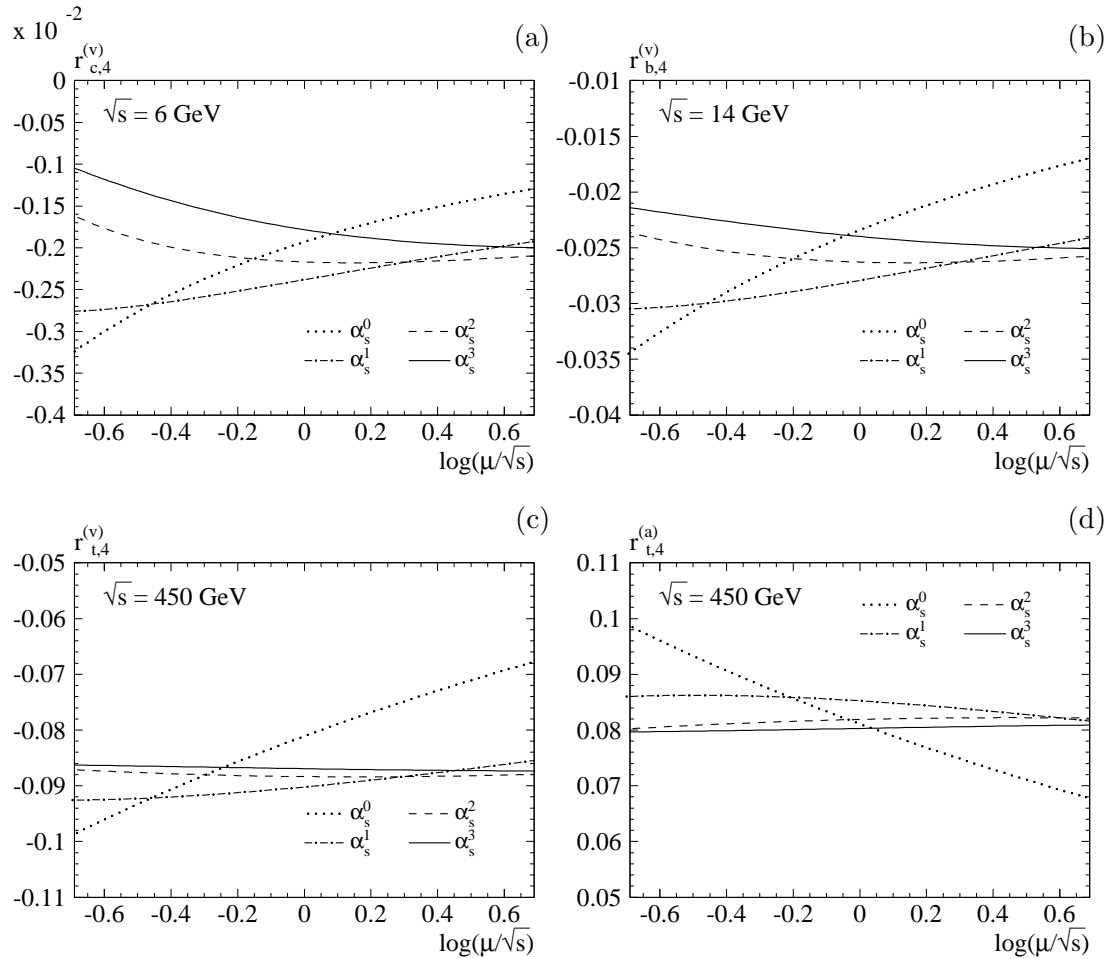


Figure 8: Variation of  $r_{Q,4}^{(v/a)}$  with  $\mu$ . Conventions as in Fig. 7.

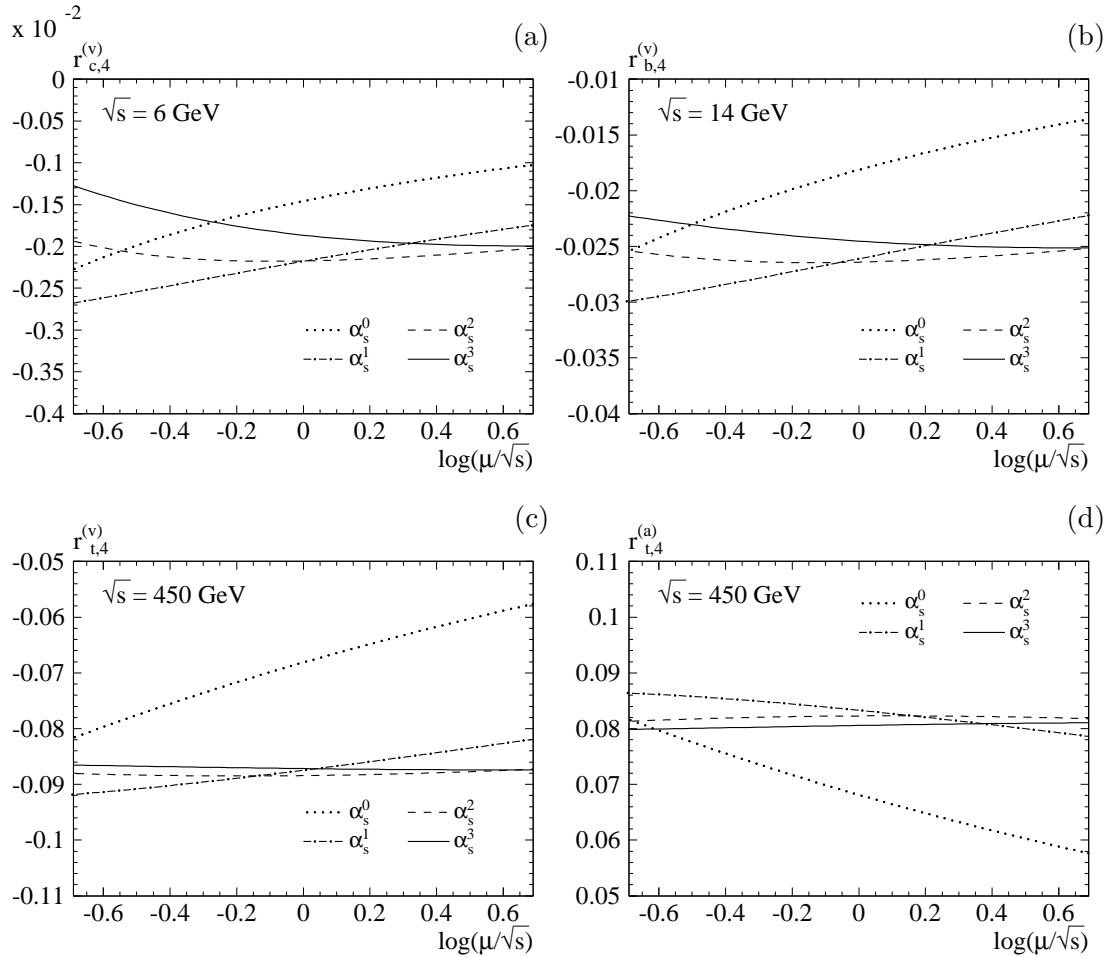


Figure 9: Variation of  $r_{Q,4}^{(v/a)}$  with  $\mu$ , using the invariant mass  $\hat{m}$ . The conventions are the same as in Fig. 7 and 8.